International Journal of Engineering Works
Kambohwell Publisher Enterprises
ISSN: 2409-2770 Vol. 5, Issue 2, PP. 32-36, February 2018
www.kwpublisher.com

A Novel Method for Insulation Testing of High Voltage Electrical Equipment

Taimur Khan, Adnan Haleem

Abstract—Different equipment's are used to test the insulation of electrical machines and measure the break down voltages of different materials, e.g. Rogowski Profile, Borda Profile and fluke insulation tester. These testing techniques works on a common principle of applying a very high voltage across the insulating material and keep increasing the voltage which increases the electric field until the breakdown voltage is reached where the insulation breaks down. Different materials are tested via insulation testers to determine their breakdown voltages so that the corresponding correct materials are used accordingly in different situations. Devices with higher impurities causes sparks and arcing, so dielectrics having higher breakdowns should be used as their insulation, otherwise, a suitable dielectric should be used. This paper offers a novel method to overcome the above-mentioned problems using an insulation testing device that should be automated, less bulky, less expensive, portable and which shall be easy to use with higher degree of safety.

Keywords— A.C., D.C., CT, SA, HTS, HV, FBT, LOPT

I. INTRODUCTION

The potential benefits of electrical energy supplied to a number of consumers from a common generating system were recognized shortly after the development of the 'dynamo', commonly known as the generator. The first public power station was put into service in 1882 in London (Holborn). Soon several other public supplies for electricity followed in other developed countries. The early systems produced direct current at low-voltage, but their service was limited to highly localized areas and were used mainly readily apparent. By 1890 the art in the development of an A.C. generator and transformer for electric lighting. The limitations of D.C. transmission at low voltage became had been perfected to the point when A.C. supply was becoming common, displacing the earlier D.C. system. The first major A.C. power station was commissioned in 1890 at Deptford, supplying power to central London over 28 miles at 10kV. Although the majority of the world's electric transmission is carried on A.C. systems, high voltage direct current (HVDC) transmission by overhead lines, submarine cables, and back to-back installations provides an attractive alternative for bulk power transfer. HVDC permits a higher power density on a given right-of-way as compared to A.C. transmission and thus helps the electric utilities in meeting the environmental requirements imposed on the transmission of electric power. HVDC also provides an attractive technical and economic solution for interconnecting asynchronous A.C. systems and for bulk power transfer requiring long cables. [1]

Taimur Khan: was with Bahria University Islamabad, Pakistan and currently employed as an E/M Engineer at Pakistan Civil Aviation Authority, Peshawar. (email: taimur1358@gmail.com)

II. EXISTING TECHNIQUES FOR HIGH VOLTAGE MEASUREMENT

This research paper presents the operating principle, design, and testing of a coaxial D-dot (the time derivative of electric flux density) probe to measure fast-front high voltages, e.g., the residual voltages of surge arresters (SAs). This probe consists of three identical copper toroid's placed around a high-voltage electrode, where all are coaxially assembled in a large earthed cylinder.

The probe was first simulated by a finite-element package to optimize the assembly and reduce the electric field inside it. This was confirmed by an alternating current test to ensure a corona-free design. Simultaneous impulse voltage measurements were done using the designed D-dot probe – two commercial mixed resistive-capacitive (RC) probes and a damped capacitive voltage divider.

The linearity of the D-dot probe was checked under unloaded and loaded conditions. Results reveal that the larger the toroid separation and/or the lower the attenuator capacitance is, the higher the measured voltage from the middle "signal" toroid will be. The residual voltage waveforms for an 11-kV SA, measured by two commercial mixed RC-probes and the damped capacitive voltage divider, showed an initial inductive overshoot superimposed on the waveform and a significant decay, even before the current peak instant [3].

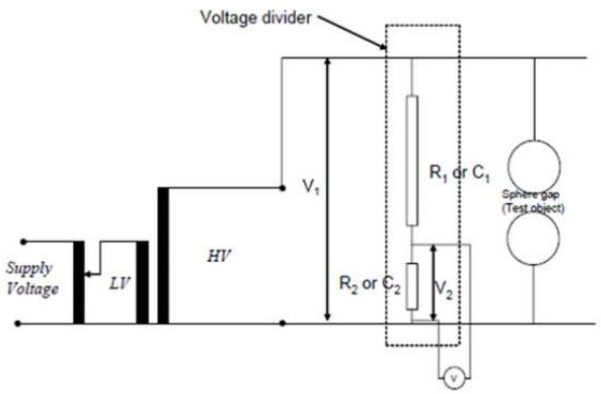

Figure 1. Schematic diagram of a typical A.C test transformer

On the contrary, the voltage measured by the designed D-dot probe gave a voltage waveform that looked like that of the current and slightly led the latter. For the damped capacitive voltage divider and the two commercial mixed RC probes, neither the peak voltage nor the voltage at peak current gave the correct current-voltage characteristics. This confirms the contradiction of some published SA models in the high-conduction regime because most models were based on measurements done by different and large-impulse capacitive or resistive voltage dividers with improper compensation. Fig.1. shows the schematic diagram of a typical AC test transformer and its connections.

The development of high superconductors (HTS) has now reached the stage where their application in power system equipment is in the process of being implemented. Consequently, there is a need to investigate the properties and applicability of high voltage insulation at cryogenic temperatures. This paper will examine the insulating materials being used at such temperatures and the dielectric properties of such materials. A major factor in the deterioration of electrical insulation at normal operating conditions is the insulation temperature and there is a well-developed understanding of the aging characteristics under such temperature conditions. However, at cryogenic temperatures the properties of insulation under high electric stress may be quite different than the case for conventional operating temperatures and the aging process may be substantially altered. There is thus a need to investigate the insulation properties at cryogenic temperatures. This paper reviews the test methods for condition monitoring of insulation under such conditions and reports the first part of experimental results at ambient condition. The results obtained and further study at cryogenic temperature will provide necessary information for design of new HTS equipment. Fig.1. shows insulation resistance values for HV cable. [4]

TABLE I. INSULATION RESISTANCE VALUES FOR HV CABLES

Cable Rated Voltage	MINIMUM IR @ 1KV DC NEW CABLE	Minimum IR @ 500V Screen-E	Minimum IR @ 1KV DC Existing Cable	Minimum IR @ 500V Screen-E Existing Cable
11 KV	400 MOhm	100 MOhm	100 MOhm	1.0 MOhm
22 KV	400 MOhm	100 MOhm	100 MOhm	1.0 MOhm
33 KV	800 MOhm	100 MOhm	200 MOhm	1.0 MOhm
66 KV	800 MOhm	100 MOhm	200 MOhm	1.0 MOhm
132 KV	800 MOhm	100 MOhm	200 MOhm	1.0 MOhm

The minimum values for IR tests vary depending on the type of equipment and the nominal voltage. They also vary according to international standards. Some standards will define the minimum IR test values for the general electrical installations. In the ANSI/NEC world, the standard provides test procedures and acceptance levels for most types of electrical equipment. [5] Fig.II provides representative acceptance values for IR test measurements, which should be used in the absence of any other guidance.

TABLE II. IR TEST VOLTAGE FOR ELECTRICAL EQUIPMENT

Maximum Voltage Rating of Experiment	**MINIMUM DC TEST VOLTAGE**	**Insulation Resistance Test Voltage for Electrical Apparatus**
250 V	500 V	25 MOhm
600 V	1000 V	100 MOhm
5000 V	2500 V	1000 MOhm
8000 V	2500 V	5000 MOhm
15000 V	2500 V	20000 MOhm

III. FLOW CHART

A flow chart is developed for the project as shown in Fig.2. The flow chart is initiated using the Remote-Control which will send signals to the Receiver Section using Bluetooth. The microcontroller used at receiver's side will generate the desired frequency, vary the voltage supplied to the primary side of the ferrite core transformer, as a result, the secondary voltage from the ferrite core transformer will be supplied to the electrode that will be used for testing. The secondary voltage available at the electrodes will be monitored using CT and optocoupler circuit and as the spark occurs across the spark gaps breakdown voltage will be displayed on LCD in Receiver Section.

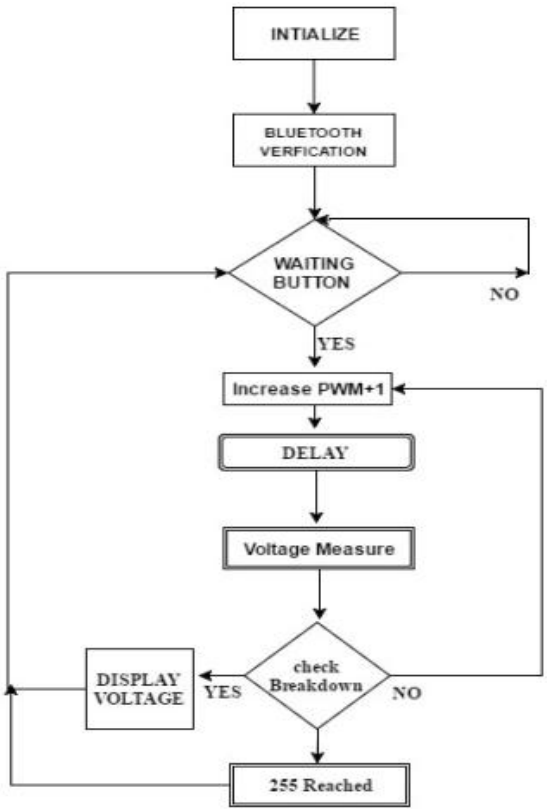

Figure 2. Flow Chart of Insulation Situation Analysis

ISSN: 2409-2770

IV. BLOCK DIAGRAM

The block diagram developed for the project is shown in Fig.3

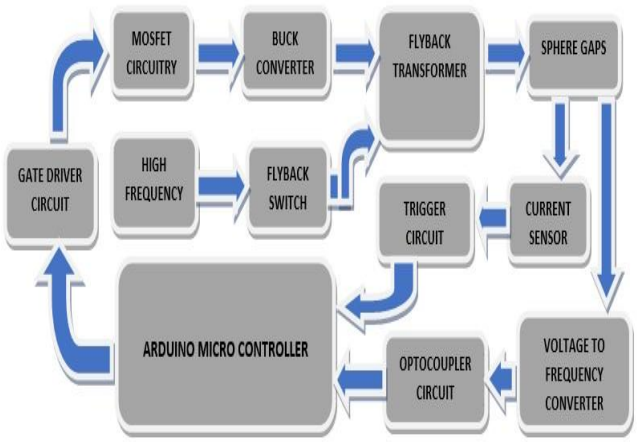

Figure 3. Block Diagram

V. MATHEMATICAL MODELLING

A voltage mode PWM controller(SG3525) is used as DC to DC converter for controlling the output voltage as well as for switching ON/OFF MOSFET(80NF70). PWM signals of different duty cycle (0-98%) will be provided to buck converter. As it will be pulsating DC so buck converter will make it a pure DC, that voltage will be supplied to the primary side of the Fly-back transformer, whereas, the secondary voltage will be provided to the spark gaps, with a voltage divider connected in parallel. The output of the voltage divider is provided to the voltage to frequency converter (LM331 IC), the output frequency of which will be interpreted by the Photocoupler (4N25) and read by the Arduino Microcontroller and the corresponding voltages via bluethooth module (HC06) will be displayed on LCD (16x2 Matrix).

Selecting Frequency of IC SG3525

A Fly-back transformer typically operates with switched currents at much higher frequencies in the range of 15 kHz to 50 kHz and it is used extensively in switched-mode power supplies for both low (3 V) and high voltage (over 10 kV) supplies. A high frequency driver is required to drive the fly-back transformer, for that, an IC SG3525 is used in the circuitry. Its main function is to either increase or decrease the duty cycle depending on the voltage levels on inverting and non-inverting inputs (Pin 1 and 2). The frequency of PWM is dependent on timing capacitance(CT) and timing resistance(RT). The deadtime resistance(RD) also slightly affects the frequency. The frequency is related to CT, RT and RD as follow,

$$f = \frac{1}{C_T (0.7 R_T + 3 R_D)} \quad \text{....[8]}$$

Where,
R_T is in the range of 2KΩ to 150 KΩ,
C_T must be in the range of 1nF to 0.2µF, and
R_D is in the range between 10Ω to 47Ω.

Taking CT as 1.4x 10–9F, RD as 40Ω and RT as 6000Ω, So, frequency (f) comes out to be 17Khz which is supplied to Fly-back transformer.

Calculation for Ferrite Core Fly-back Transformer

A flyback transformer (FBT), also called as a line output transformer (LOPT), generate high voltage sawtooth signals at a relatively high frequency. The primary turns for this project are calculated using the formula,

$$N_{pri} = \frac{V_{in(nom)} \cdot 10^8}{4 \cdot f \cdot B_{max} \cdot A_c} \quad \text{....[9]}$$

Where, Vin(nom) is the nominal input voltage usually taken as 12V, f is the operating switching frequency (Hz) which is taken as 16.5-17 Khz, Bmax is the maximum flux density in Gauss (taken between 1300-2000G) and Ac is the effective cross-sectional area in cm2 (For ETD39 it is 1.25cm2). The primary turns calculated are 9 and are wounded on primary end of ferrite core transformer as shown in Fig.4.

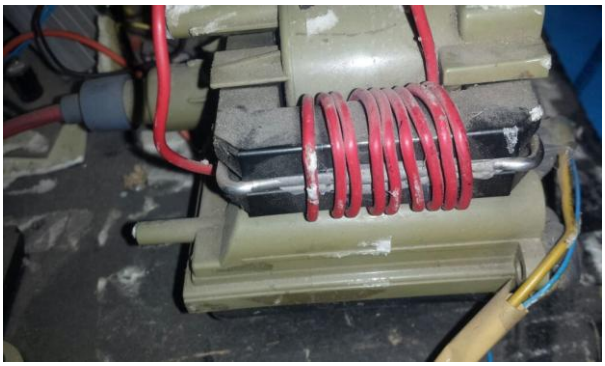

Figure 4. Primary turns of the Ferrite Core Transformer

Now the voltage ratio is calculated using formula,

Vratio=Vs/Vp =16.5KV/12V =1375V

Knowing the Secondary to Primary voltage ratio we can now easily calculate the Secondary turns of the Fly-back transform--er,

Nratio = Ns/Np = Ns/9

Finding frequency of IC LM331

The LMx31 family of voltage-to-frequency converters are ideally suited for use in simple low-cost circuits for analog-to-digital conversion, precision frequency-to-voltage conversion, long-term integration, linear frequency modulation or demodulation, and many other functions. The output when used as a voltage-to-frequency converter is a pulse train at a frequency precisely proportional to the applied input voltage whose frequency can be calculated using the formula,

Fout = (Vin / 2.09V) × (Rs/Rl) × (1/(Rt × Ct))

ISSN: 2409-2770

To keep the same linearity as before with the frequency to voltage conversion stage, Rs = Rl = 100 KΩ, hence Rs/ Rl = 1. The parameter V is the same as before, which is 12 volts.The timing value of the resistor Rt = 4 KΩ, and capacitor Ct = 0.01 µF, Hence, the equation simplifies to that shown below.

$$Fout = 996.81 \times Vin\ Hz$$

This Vin is provided using a Voltage divider circuit.

Calculation for Voltage divider circuit

A typical voltage divider circuit is used, the formula for which is,

$$V_{out} = \frac{R_2}{R_1 + R_2} \cdot V_{in}$$

Where, R1=194MΩ, R2=84KΩ and Vin=2310.524V, So Vout is equal to 1V.

Response of Remote Section

From the above calculation, it can be concluded that as the Voltage(Vout)=1V is received by the remote section via Bluetooth, the remote section will display a value of 2310.524V.

System Model of the Project

This system model of the project comprises of two sections. A Remote-Control Section and a Receiver Section. The Remote-Control section comprises of an Arduino microcontroller that uses Bluetooth technology to remotely connect to the Receiver connection and thus provide portability and high degree of Safety. The Receiver Section comprises of a Buck converter, Ferrite Core transformer, Gate driver and MOSFET circuitry, two Sphere Gaps, CT and an Optocoupler circuit for voltage sensing and an Arduino microcontroller which controls the Receiver Section and communicates with the Remote-Control section. Both the section was successfully simulated in Proteus Software as shown in Fig.5.

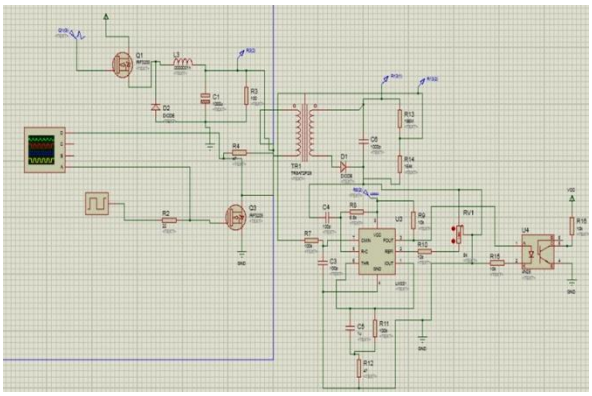

Figure 5. System Model in Proteus Software

VI. SIMULATION

A PWM signals of different duty cycle from will be given to buck converter. As it will be pulsating DC so that voltage will be given to buck converter to make it pure DC. That voltage will be supplied to the primary side of the fly back transformer. The voltage at secondary side will be given to spark gaps. Voltage divider is connected in parallel with spark gaps, LM331 IC will change voltage into frequency and then this frequency will be read by Arduino Micro Controller and voltage value will be shown on LCD connected at remote side. When voltage across the spark gaps reaches the breakdown voltage of an insulator placed in between the spark gaps a flash over will happens due to flash over current will increase and that current will be sensed by Current transformer. [6] Current transformer will give signal to Microcontroller to stop the generation of PWM signal LM331 IC will convert the breakdown voltage into frequency, this frequency via Photo coupler will be sent to and interpreted by the Arduino Micro Controller. Fig.6. shows the simulation results as on digital oscilloscope which clearly indicate that the Input wave (Yellow) is much smaller as compared to the output wave (Green) of a fly back transformer.

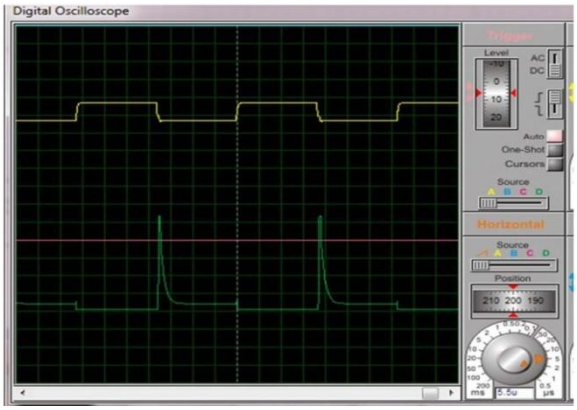

Figure 6. Simulation Results on Digital Oscilloscope

VII. HARDWARE MODELLING

The hardware model comprises of a fully populated Arduino board which connects the LCD to the Arduino as well as shown in Fig.7. A pair of spark gaps which consists of a two electrodes separated by a gap usually filled with air, fully assembled, All the PCBs are attached to the acrylic sheet through nuts and bolts The two male pin header connectors which are connected to the CT board and Triac switch board through IDE cable, as shown in Fig.6.

Figure 7. Remote Connectivity and Display Module

ISSN: 2409-2770

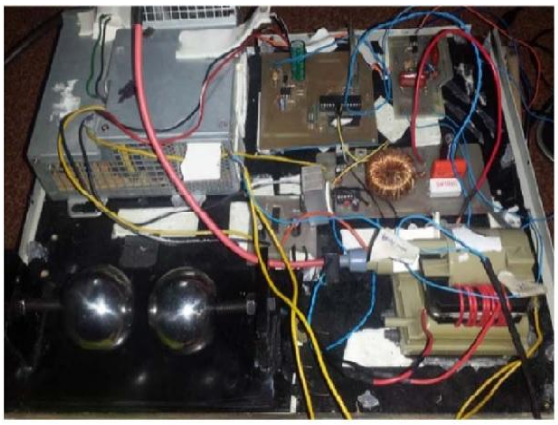

Figure 8. Hardware Model of the Project

VIII. RESULTS

Breakdown Voltage for Air

The breakdown voltage of air was tested with different air gaps between the electrodes and it is observed that as the air gap increases, the breakdown voltage increases. [7] Fig. 4 shows air breakdown voltages at different gap distance but after certain gap distance, the device stops measuring the voltage. The reason is that gap length exceeds the device measuring
capacity.

TABLE III. BREAKDOWN VOLTAGE OF AIR AT DIFFERENT GAP DISTANCES

BREAKDOWN VOLTAGE (KV)	**SPHERE GAP DISTANCE (MM)**
5	1
10	2.6
15	4.2
20	5.8

Breakdown Voltage for Solid Insulators

The Breakdown voltage of other insulations such as paper, rubber, and hardboard breakdown can also be measured with this device Fig. 5 shows the breakdown voltage of solid insulators.

TABLE IV. BREAKDOWN VOLTAGE OF SOLID INSULATORS

INSULATING MATERIAL	BREAKDOWN VOLTAGE (KV)
A4 Paper	0.8
Chart Paper	2
Hard Board	2.6
Rubber	11
Wood	16

CONCLUSION

In this paper, the breakdown voltage of Air and other solid insulators was investigated. The experimental results confirmed that the impact of the barrier is dependent on the air gap length. Also, the results highlight the effect of physical characteristics of the dielectric barriers in the breakdown voltage enhancement. Finally, we used the experimental results that were carried out in the high voltage laboratory to validate the hardware model. The study shows that the results were in good agreement with the experimental results.

REFERENCES

[1] I. A. Metwally, "-Dot Probe for Fast-Front High-Voltage Measurement," in *IEEE Transactions on Instrumentation and Measurement*, vol. 59, no. 8, pp. 2211-2219, Aug. 2010.doi: 10.1109/TIM.2009.2030928

[2] T. R. Blackburn, C. Grantham, B. T. Phung, Z. Y. Liu, M. F. Rahman and J. X. Jin, "High voltage insulation test for high Tc superconducting types," *Applied Superconductivity and Electromagnetic Devices (ASEMD), 2013 IEEE International Conference on*, Beijing, 2013, pp. 241-244.doi: 10.1109/ ASEMD.2013.6780753

[3] IEEE Standard Techniques for High-Voltage Testing," in *ANSI/IEEE Std 4-1978* , vol., no.,pp.0_1-,1978doi:10.1109 / IEEESTD.1978.119190

[4] D. Pan, H. W. Li and B. M. Wilamowski, "A low voltage to high voltage level shifter circuit for MEMS application," *University/Government/Industry Microelectronics Symposium, 2003. Proceedings of the 15th Biennial*, 2003, pp. 128-131. doi: 10.1109/UGIM.2003.1225712

[5] R. R. M. Pendor, Z. Abas and A. K. Yahya, "Winchester-Banana platform for high temperature and high-voltage reliability testing with voltage monitoring capability," *36th International Electronics Manufacturing Technology Conference*, Johor Bahru, 2014, pp.1-7.doi: 10.1109 /IEMT.2014.7123113

[6] K. A. O'Connor and R. D. Curry, "High voltage characterization of high dielectric constant composites," *2010 IEEE International Power Modulator and High Voltage Conference*, Atlanta,GA,2010,pp.159-162.doi: 10.1109 /IPMHVC.2010.5958318

[7] R. Minkner, "Development trends in medium- and high voltage technologies for measuring systems, filters and bushings," *Power Tech, 2005 IEEE Russia*, St. Petersburg, 2005,pp.1-8.doi: 10.1109/PTC.2005.4524818.

[8] M. S. Naidu and V. Kamaraju, High Voltage Enginnering, Tata McGraw-Hill 2004.

[9] E. Kuffel, W. S. Zaengl, and J. Kuffel, High Voltage Engineering. Fundamentals, Butterworth-Heinemann, 2nd edition, 2000.